Available online at www.sciencedirect.com
ScienceDirect
Micron xxx (2007) xxx–xxx
micron
www.elsevier.com/locate/micron

Review

Structural analysis of hydrophobins

Margaret Sunde [a], Ann H.Y. Kwan [a], Matthew D. Templeton [b], Ross E. Beever [c], Joel P. Mackay [a,*]

[a] *School of Molecular and Microbial Biosciences, University of Sydney, Sydney 2006, Australia*
[b] *The Horticultural and Food Research Institute of New Zealand, Mt Albert Research Centre, Auckland, New Zealand*
[c] *Landcare Research, Tamaki Campus, Auckland, New Zealand*

Received 25 June 2007; received in revised form 7 August 2007; accepted 7 August 2007

Abstract

Hydrophobins are a remarkable class of small cysteine-rich proteins found exclusively in fungi. They self-assemble to form robust polymeric monolayers that are highly amphipathic and play numerous roles in fungal biology, such as in the formation and dispersal of aerial spores and in pathogenic and mutualistic interactions. The polymeric form can be reversibly disassembled and is able to reverse the wettability of a surface, leading to many proposals for nanotechnological applications over recent years. The surprising properties of hydrophobins and their potential for commercialization have led to substantial efforts to delineate their morphology and molecular structure. In this review, we summarize the progress that has been made using a variety of spectroscopic and microscopic approaches towards understanding the molecular mechanisms underlying hydrophobin structure.

Keywords: Hydrophobin; Amphipathic; Biofilm; Rodlet; Monolayer; NMR; Self-assembly; X-ray diffraction

Contents

* Corresponding author. Tel.: +61 2 9351 3906; fax: +61 2 9351 4726.
E-mail address: j.mackay@mmb.usyd.edu.au (J.P. Mackay).
URL: http://www.mmb.usyd.edu.au/mackay/

0968-4328/$ – see front matter
doi:10.1016/j.micron.2007.08.003

Please cite this article in press as: Sunde, M., et al., Structural analysis of hydrophobins, Micron (2007), doi:10.1016/j.micron.2007.08.003

1. Introduction

1.1. Discovery of hydrophobins

Hydrophobins are a family of low molecular weight proteins with a characteristic pattern of cysteine residues that form four disulphide bonds (Fig. 1). Aside from the cysteines, hydrophobins otherwise share little amino acid sequence homology but do show very similar hydrophobicity plots. They were named hydrophobins by Wessels and co-workers during studies of genes that are highly expressed during fruit body formation of the mushroom-like fungus *Schizophyllum commune* (Dons et al., 1984; Wessels et al., 1991). Subsequently, it was shown that products of one such gene (SC3) possessed the remarkable property of spontaneously polymerising at gas–water interfaces into SDS-insoluble amphipathic sheets with the highly hydrophobic surface facing the gas and the hydrophilic surface facing the water (Wösten et al., 1993; Wösten, 2001). Under transmission electron microscopy (TEM) these sheets comprised regular arrays of microfibrils, closely resembling the rodlet layers recognised on the cell surface of many dry-spored mould fungi (Hess et al., 1968; Hess et al., 1969; Dempsey and Beever, 1979) (Fig. 2). The role of these rodlet layers in conferring hydrophobicity to such dry spores was demonstrated by the finding that the *eas* mutant of the dry-spored *Neurospora crassa* lacked the rodlet layer (Beever and Dempsey, 1978).

Analysis of the soluble hydrophobin protein product was initially hindered by the insolubility of the rodlet layers, which cannot be dissolved by organic solvents, hot detergent or treatment with alkali (Beever et al., 1979). The discovery that the polymers could be dissolved in 100% trifluoroacetic acid (de Vries et al., 1993; Wösten et al., 1993), and that the purified hydrophobin protein could subsequently be repolymerised into rodlets, paved the way for the analysis of the soluble forms of class I hydrophobins (see Section 3). Subsequently, hydrophobins have been identified in many groups of fungi and correlation of the protein sequences from a number of hydrophobins with their observed physical properties revealed two classes (Wessels, 1994). Class I hydrophobins form highly insoluble polymers that have the appearance of distinct rodlets, whereas class II hydrophobins form polymers that are soluble in some organic solvents and lack the rodlet appearance of class I hydrophobins (Yaguchi et al., 1993; Wösten and de Vocht, 2000; Paananen et al., 2003). In addition, class II hydrophobins have hydrophobicity plots that are distinct from the class I proteins. They also display far greater conservation in the spacing of amino acids between the cysteine residues than do class I hydrophobins (Linder et al., 2005).

1.2. Hydrophobin encoding genes

Hydrophobins are unique to the fungal kingdom, although there are functional homologues in the Streptomycetes (chaplins), and the dimorphic yeast *Ustilago maydis* (repellents) (Wessels et al., 1991; Wessels, 1996; Claessen et al., 2003; Teertstra et al., 2006). Analysis of completed fungal genomes indicate that hydrophobins exist as small gene families of between two and seven members in most species, with the exception of the mushroom *Coprinus cinereus* which has 23 genes (http://www.broad.mit.edu/). Since *C. cinereus* is the only mushroom whose genome sequence has been completed, it is possible that this number of hydrophobin encoding genes may be typical of mushrooms. Hydrophobin genes have not been annotated from the genome sequences of zygomycetes and chytrids (http://www.broad.mit.edu/) although polymeric rodlet-like structures have been observed

Fig. 1. Amino acid sequence comparison of class I and II hydrophobins. Only amino acids between the first and last Cys residues are shown due to high sequence variations at the termini. The conserved Cys residues are highlighted in yellow with the conserved disulphide bonding pattern indicated with brackets. The relatively low degree of sequence conservation is apparent. The abbreviations used are: SC3, *S. commune* (accession P16933); SC4, *S. commune* (accession P16934); EAS, *N. crassa* (accession Q04571); MPG1, *M. grisea* (accession P52751); HCF1, *C. fulvum* (accession Q00367); ABH1, *A. bisporus* (accession P49072); PRI2, *A. aegerite* (accession Q9Y8F0); RODA, *A. fumigatus* (accession P41746); HFBI, *T. reesei* (accession P52754); HFBII, *T. reesei* (accession P79073); CU, *O. ulmi* (accession Q06153); CRP, *C. parasitica* (accession P52753); HCF6, *C. fulvum* (accession Q9C2X0); MGP, *M. grisea* (accession O94196); HYD4, *G. moniliformis* (accession Q6YF29) and SRH1, *T. harzianum* (accession P79072).

Please cite this article in press as: Sunde, M., et al., Structural analysis of hydrophobins, Micron (2007), doi:10.1016/j.micron.2007.08.003

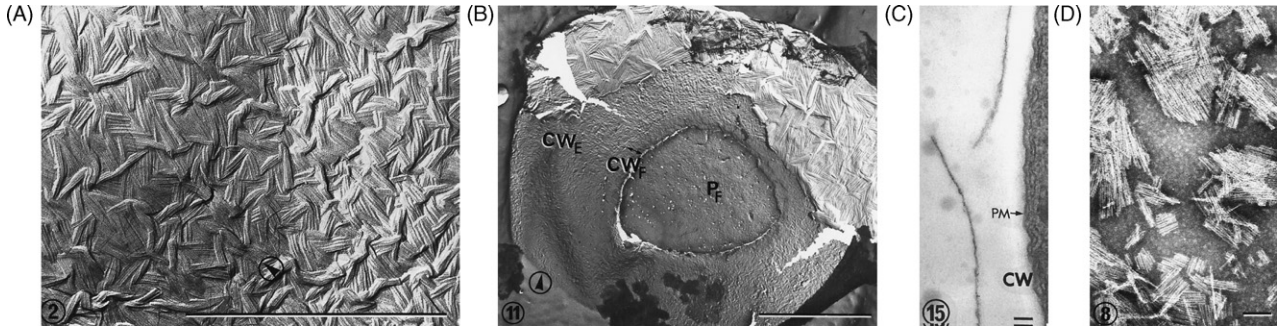

Fig. 2. TEM images of *N. crassa* spore surface. (A) Carbon shadowed platinum replica, bar 1 mm. (B) Deep-etch of freeze-fractured *N. crassa* conidium, the initial fracture passed through the cell wall (CW_f) and then along the plasma membrane revealing the P_f face. Etching then exposed the outside of the cell wall (CW) and shows that in some regions the cell wall is covered by rodlets, bar 1 mm. (C) TEM of spores surface showing rodlet layer, bar 0.1 μm. (D) Negative stain of rodlet layer purified form spores, bar 0.1 μm. Reproduced with permission from Dempsey and Beever (1979), Copyright 1979, American Society for Microbiology.

on the spores of the zygomycete *Syncephalastrum racemosum* (Hobot and Gull, 1981), suggesting that related genes do exist in these fungi.

1.3. Role of hydrophobins in the fungal life style

Fungi are heterotrophic, predominantly terrestrial organisms that are critical in organic matter breakdown and nutrient recycling. They exhibit two main growth morphologies. The growth unit in filamentous fungi (fungi *sensu stricto*) is an apically growing branching tube (the hypha), which in macroscopic species aggregates into large fruiting bodies such as mushrooms. In contrast, yeasts, which have evolved independently in both major fungal groups (the frequently microscopic ascomycetes and the frequently macroscopic basidiomycetes), grow as budding unicells in generally aqueous habitats. To date, while highly annotated genomes are available for a number of yeasts, no hydrophobins have been recognised, suggesting that they are dispensable for growth in such habitats.

Fungi grow on and within organic substrates, primarily the dead and living tissues of macro-organisms. Whereas the surface of the hypha wall growing in a moist substrate is hydrophilic, the cell wall surface of aerial hyphae and airborne spores is hydrophobic. This fundamental change in the surface properties of the cell wall is achieved through the secretion of hydrophobins (Wessels, 1996; Wösten, 2001). Hydrophobins act as natural surfactants and reduce the surface tension of the growth medium, thus allowing fungi to breach the water–air interface and to produce aerial structures such as hyphae (Wösten et al., 1999). Similarly, the spores that develop on the end of the aerial structures are coated by an amphipathic hydrophobin layer that renders their surface hydrophobic and resists wetting, thus facilitating effective dispersal in air. While the hydrophobin layer is strongly hydrophobic, acting to prevent water penetration and consequent water logging, it is nevertheless highly permeable to gas exchange (Wang et al., 2005), behaving in a manner resembling GORE-TEX™.

While many fungi grow on dead tissues, a large number also grow in close symbiotic relationships with other living organisms, both as pathogens and mutualists. Hydrophobins have been found to play important roles in such interactions. Gene-knockout of *MPG-1*, a class I hydrophobin from the rice blast fungus *Magnaporthe grisea*, reduced appressorium formation and hence pathogenicity, in addition to conferring the easily wettable phenotype (Talbot et al., 1996). *MHP-1*, a class II hydrophobin from the same fungus, was also found to be highly expressed during both conidiation and pathogenesis. The mycelia of knock-outs of *MHP-1* expressed a detergent-wettable phenotype, in a similar fashion to *DewA* in *Aspergillus nidulans* (Stringer et al., 1991). Furthermore, the knock-outs were less pathogenic and produced fewer conidia (Kim et al., 2005). In contrast, disruption of *HCf-1* or *HCf-6*, class I and class II hydrophobins, respectively from *Cladosporium fulvum*, does not reduce pathogenicity (Spanu, 1998; Whiteford and Spanu, 2001; Whiteford et al., 2004). Similarly, whereas the class II hydrophobin cerato-ulmin from the Dutch elm disease fungus *Ophistroma ulmi* is strongly phytotoxic, the protein is not essential for pathogenicity (Brasier et al., 1995; Bowden et al., 1996). The critical role of cerato-ulmin may be in dispersal by facilitating attachment of spores to the insect vector (Temple and Horgen, 2000). Cryparin, a class II hydrophobin from the chestnut blight fungus *Cryphonectria parasitica*, has been shown to be important for stromal pustule eruption (Kazmierczak et al., 2005).

Genes that encode hydrophobins have also been cloned from lichens and rodlets have been observed in the internal airspaces that are vital for efficient gas exchange (Scherrer et al., 2000), where they probably play a key role in preventing these internal airspaces from collapsing. High levels of hydrophobin expression have been observed in ectomycorrhizal fungi in symbiotic associations with plant roots, where they may also be involved in maintaining gaseous exchange (Martin et al., 1995; Tagu et al., 1998; Martin et al., 1999; Tagu et al., 2002). As well as their multifarious roles in association with living fungi, hydrophobins may have additional far reaching roles in terrestrial ecosystems through their roles in soil. For example, it has been suggested that hydrophobic patches in soils, which prevent water penetration may be due to the presence of hydrophobins (Rillig, 2005).

1.4. Biotechnological applications for hydrophobins

More recently, research on hydrophobins has focussed on utilising their unique physical properties for biotechnological applications. Efforts include modification of either hydro-

phobic surfaces such as Teflon, or hydrophilic surfaces such as mica, to facilitate the attachment of enzymes or other proteins (Qin et al., 2007). Treatment of petri dishes with the class I hydrophobin SC3 fused to fibronectin enables human cell cultures to grow, suggesting the construct might be capable of making implant surfaces more biocompatible (Janssen et al., 2004). Hydrophobins have also been used to attach enzymes to electrodes to improve the efficiency of biosensors (Zhao et al., 2007), as well as to immobilise fusion partner proteins to hydrophobic surfaces (Linder et al., 2002). A related application is the use of hydrophobins as fusion tags for the purification of recombinant proteins using aqueous two-phase systems (Linder et al., 2004). Further, it has been suggested that hydrophobins can stabilize emulsions and might therefore have a wide range of applications such as acting as surfactants and emulsifiers in processed foods and cleaning agents (Linder et al., 2005).

2. Immunological and fluorescence localization of hydrophobins *in situ*

During development, expression of hydrophobin-encoding genes is regulated in a temporal manner (Stringer et al., 1991; Bell-Pedersen et al., 1992) and where gene families have been described, family members tend to be differentially expressed (Scherrer et al., 2002; Trembley et al., 2002; Whiteford et al., 2004). In contrast, relatively little is known about the spatial regulation of hydrophobin expression. SC3 from *S. commune* grown in submerged culture has been shown to be secreted into the medium at hyphal apices, whereas in emerging hyphae SC3 accumulates on the hyphal surface and mediates attachment to hydrophobic surfaces (Wösten et al., 1994). In contrast, immunogold localisation of SC4, also from *S. commune,* and ABH-1 from *Agaricus bisporus* has shown that these hydrophobins specifically line the air channels of the mushroom (Lugones et al., 1999). Similarly, DGH-1 from *Dictyonema glabratum* has been shown to line the air cavities in lichens (Trembley et al., 2002).

An alternative approach to defining the *in planta* localization of hydrophobin expression in the plant pathogenic fungus *Cladosporium fulvum* was taken by Whiteford and co-workers (Whiteford et al., 2004). They fused the V5 antibody epitope to the C-terminus of both HCf-1 (a class I hydrophobin) and HCf-6 (class II) and monitored their spatial localisation. HCf-1 was localized both to the surface of conidia and to aerial hyphae that emerged through stomata from the infected leaf. In contrast the class II hydrophobin HCf-6 was not present on conidia or emergent hyphae but was found on infection hyphae and was secreted *in planta* (Whiteford et al., 2004). The distinct temporal and spatial expression of different members of hydrophobin gene families indicates the possibility of functional specialisation. Indeed, hydrophobins have been shown to be important for various fungal morphogenetic processes (Kershaw and Talbot, 1998; van Wetter et al., 2000). However, such issues are unlikely to be satisfactorily resolved until we know more about the structure and assembly of hydrophobin monolayers.

3. Structural studies of hydrophobins in non-assembled forms

In order to gain insight into hydrophobin structure and the formation of polymerised films, two complementary approaches can be taken. One can characterise the structure of non-assembled hydrophobins (this section) and one can also examine assembled monolayer films using microscopic techniques; this latter strategy is reviewed in Section 4. Ultimately, it is hoped that these two approaches can be brought together to provide a complete molecular description of hydrophobin structure and assembly.

3.1. Circular dichroism spectropolarimetry and infra-red spectroscopy

The secondary structure content of the class I hydrophobin SC3, from the wood-rotting fungus *Schizophyllum commune,* has been extensively studied using circular dichroism spectropolarimetry (CD) and attenuated total reflectance Fourier-transform infra-red spectroscopy (ATR FT-IR) (de Vocht et al., 1998). Both of these methods provide a low-resolution view of the secondary structure content of a protein. The CD spectrum of soluble SC3 recorded in phosphate buffer is characteristic of a protein with elements of β-sheet structure together with some random coil. However, upon the addition of 25% trifluoroethanol (TFE, a solvent that is known to promote secondary structure formation) or colloidal Teflon, the spectrum shifted such that characteristics typical of α-helical structure started to appear. The α-helical structural elements detected in SC3 under these conditions are thought to be relevant—it has been proposed that the so-called α-helical state is an on-pathway intermediate in the SC3 assembly process (de Vocht et al., 1998, 2002; Wang et al., 2002). The CD spectra recorded of other hydrophobins including EAS, SC4, ABH3 and the class II hydrophobin cerato-ulmin in the soluble state indicated that they all contain varying degrees of β-sheet structures together with random coil regions (Yaguchi et al., 1993; Wösten and de Vocht, 2000; Mackay et al., 2001). In all cases, a significant increase in β-sheet structure is detected upon rodlet formation (Fig. 3).

The secondary structure of soluble SC3 has also been studied using ATR FT-IR spectroscopy. SC3 was dried down on a germanium plate under conditions that maintain its non-assembled state and the resulting spectrum displayed a single major amide I band at 1636 cm^{-1}. This spectrum is consistent with the presence of a mixture of secondary structure (de Vocht et al., 1998) and deconvolution and curve fitting analysis of the band estimated that soluble SC3 is composed of 23% α-helix, 41% β-sheet and 16% β-turn with the remaining 20% being random coil. Interestingly, silanization of the germanium plate to increase its hydrophobicity changed the profile obtained from soluble SC3 to one with mainly α-helix and β-sheet contributions, suggesting that these structural features might also be present in the assembling SC3 intermediates. No other examples of helical intermediates have been observed, but this might simply reflect the fact that SC3 has been studied more intensively than any other hydrophobin.

Please cite this article in press as: Sunde, M., et al., Structural analysis of hydrophobins, Micron (2007), doi:10.1016/j.micron.2007.08.003

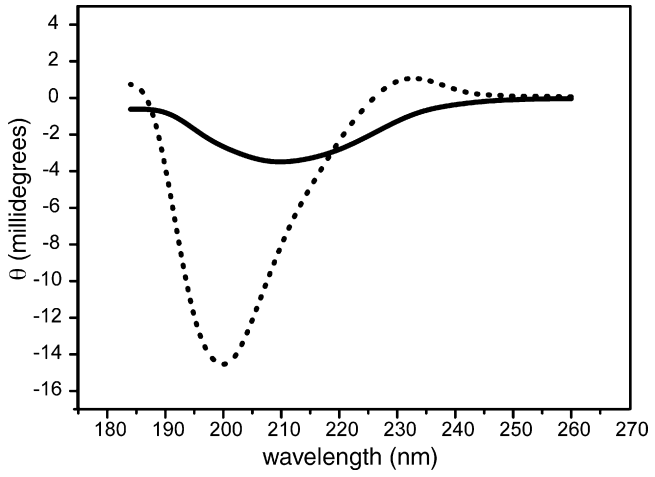

Fig. 3. Circular dichroism spectra of EAS in water (dotted line) and dried onto a quartz cuvette from water (solid line).

3.2. Peptide digestion and hydrogen/deuterium exchange

The CD and ATR FT-IR studies of SC3 and EAS suggest that a significant proportion of each protein in its soluble state has little or no secondary structure. These regions are especially interesting because they have the potential to become more ordered in the polymerised state and therefore may play pivotal roles in the self-assembly of hydrophobins. Limited proteolysis, mass spectrometry and hydrogen/deuterium (H/D) exchange measurements have been used to probe the structural features of SC3 in the soluble state as well as under conditions that are thought to mimic the polymerisation process (Wang et al., 2004). When soluble SC3 was digested with pepsin and subjected to liquid chromatography followed by mass spectrometry (LC–MS), only two peptides were detected; one of these corresponded to the predicted loop region between the third and fourth cysteine (the so-called second loop Fig. 1), suggesting this loop is exposed in soluble SC3. However, it is not clear whether the lack of signals from other regions is due solely to protection from digestion; poor ionisation in the mass spectrometer would also result in an absence of signals. Subsequent Asp-*N* digestion experiments carried out on performic acid-treated SC3 revealed that the second loop of SC3 bound strongly to colloidal Teflon and that this binding event resulted in the formation of α-helical structure as detected by CD. Furthermore, the addition of Teflon to soluble SC3 increased the protection of the second loop from pepsin digestion, consistent with results from H/D exchange experiments. These results therefore suggest the second loop is exposed in soluble SC3, undergoes a disorder to order transition during the hydrophopbin polymerisation process and is likely to play a direct role in forming the hydrophobic surface on the assembled rodlets.

3.3. X-ray crystallography

Although the low-resolution data described above have illuminated certain aspects of hydrophobin structure in specific cases, higher resolution biophysical studies have unfortunately been difficult—ironically as a consequence of the unique physical properties of these proteins. In particular, the readiness of hydrophobins to aggregate and self-polymerise, as well as the presence of substantial amounts of disorder in the soluble state, has until recently frustrated attempts to obtain crystals suitable for X-ray crystallography. Over the last 3 years however, crystal structures of the closely related class II hydrophobins HFBI and HFBII (Hakanpää et al., 2004a,b; Hakanpää et al., 2006a,b) have been determined, together with a structure of an engineered sequence variant of HFB-I (*N*-Cys HFBI; which bears an additional 13 residues at the N-terminus, PDB code 2GVM).

The crystal structures of HFBII, HFBI and its *N*-Cys variant showed that they share the same overall structure and that no other proteins in the SCOP database (other than the class I hydrophobin EAS—see below) share the same β-barrel topology (Fig. 4A–C). The hydrophobin fold is compact and globular and consists of a core β-barrel comprising of two adjoining β-hairpins. An α-helix is linked to the outside of the barrel via a disulphide bond, and another disulphide bond acts to cross-link the two strands within each of the two β-hairpins. These latter two disulphide bonds are completely enclosed by the barrel and are located on opposite ends, thereby offering high stability to the structure. The fourth disulphide bond connects the N-terminal loop to the core β-barrel.

The HFBII and HFBI structures revealed the structural basis for the high surface activity of hydrophobin molecules. The hydrophobin fold allows the display of a large flat hydrophobic patch that makes up about 20% of the total surface accessible area (in the absence of any adjacent molecules) by utilizing aliphatic side-chains located near the loop regions of the two hairpins (Fig. 4D). It is possible that the role of the disulphide bonds is in part to counteract the potentially destabilising effects of exposing such a large hydrophobic surface.

While the overall topology of HFBI and HFBII is the same, some flexibility was observed in the HFBI structure. The asymmetric unit of HFBI contains four molecules, and there is one seven-residue loop that takes up a different conformation in two of these molecules compared to the other two (Fig. 4C). This region includes some of the aliphatic residues in the hydrophobic patch, suggesting that while the β-barrel core of the hydrophobin fold is well-defined, the loop regions between the conserved cysteine residues are likely to have some flexibility. The relatively high RMSD value (2.5 Å) calculated for an overlay of the two sets of HFBI molecules within the asymmetric unit further supports the idea that, despite the presence of four disulphide bonds in such a small protein, the hydrophobin fold still appears to have a significant degree of plasticity.

3.4. Nuclear magnetic resonance (NMR) spectroscopy

The crystal structures of the class II hydrophobins HFBI and HFBII have provided valuable insights into the molecular basis for the surface properties of hydrophobins. However, in some senses the class I proteins are more striking, because of the robustness and regularity of the rodlet layer that they form. Recently, the solution structure of the class I hydrophobin

Please cite this article in press as: Sunde, M., et al., Structural analysis of hydrophobins, Micron (2007), doi:10.1016/j.micron.2007.08.003

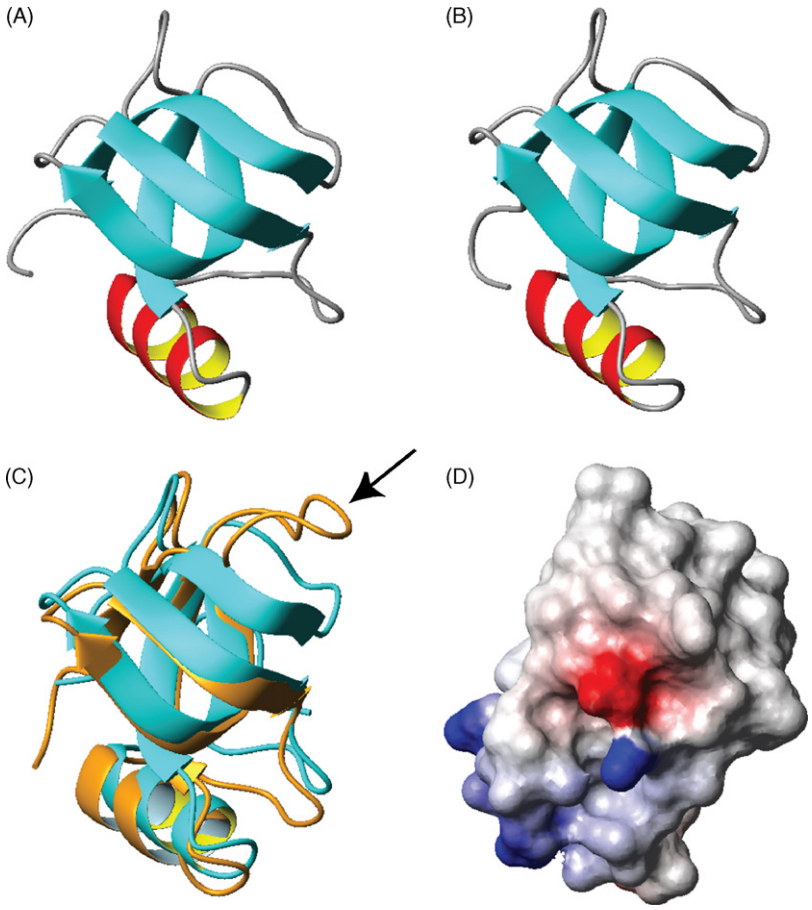

Fig. 4. The three-dimensional structures of HFBII, HFBI and its *N*-Cys variant. Ribbon diagrams showing (A) HFBII, (B) *N*-Cys HFBI, (C) a superposition of two different HFBI molecules (shown in orange and cyan) in an asymmetric unit with the flexible loop indicated by a black arrow and (D) Electrostatic surface of HFBI. Uncharged residues are shown as grey and negatively and positively charged residues are illustrated in red and blue, respectively. A large flat hydrophobic patch can be seen at the top of the molecule.

EAS was determined using triple-resonance NMR methods (Kwan et al., 2006). Like HFBI and HFBII, the core structure of EAS is centered on two interlocking β-hairpins that form a four-stranded β-barrel and display a striking segregation of charged and hydrophobic residues (Fig. 5B and C). However, in place of the α-helix found in the HFBI/II crystal structures, there is a short two-stranded antiparallel β-sheet. Apart from this, the main difference between the HFBI/II structures and EAS is that the latter contains a very long (∼24 residues) disordered loop in the region between the third and fourth Cys that is typical of class I hydrophobins but is absent in class II proteins. This loop is the least conserved portion of the class I hydrophobins in terms of both length and amino acid composition (Fig. 1). Interestingly, deletion of either 7 or 11 residues from this region yielded EAS mutants that still formed stable, well-ordered structures and retained the ability to form rodlets (Kwan et al., 2006). This supports the idea that both the hydrophobin fold and the polymeric rodlet structure must be able to accommodate significant sequence diversity in this region and explains the low apparent sequence conservation between functionally similar class I hydrophobins. A second smaller disordered region is also observed in EAS (Fig. 5A and C); the position of this loop corresponds to the flexible loop in HFBI (see above), supporting the idea that this region is indeed intrinsically flexible throughout the hydrophobin family.

4. Structural studies of the polymerised forms

The regular structure observed on fungal spores by microscopy suggests that the polymerised hydrophobin layers have an underlying, repeating order. This is particularly apparent in the rodlet layers formed by class I hydrophobins. Techniques such as electron microscopy, X-ray fibre diffraction and atomic force microscopy have been used to shed light on the structures of the polymerised hydrophobin films.

4.1. Transmission electron microscopy (TEM)

Rodlets were first observed on the outer surface of freeze-etched spores from *Penicillium* (Sassen et al., 1967; Hess et al., 1968), *Aspergillus* (Hess et al., 1969; Ghiorse and Edwards, 1973), *Oidiodendron truncatum* and *Geotrichum candidum* (Cole, 1973). However, the first detailed images and evidence of their function were not provided until the appearance of three papers in 1978–9 (Beever and Dempsey, 1978; Beever et al.,

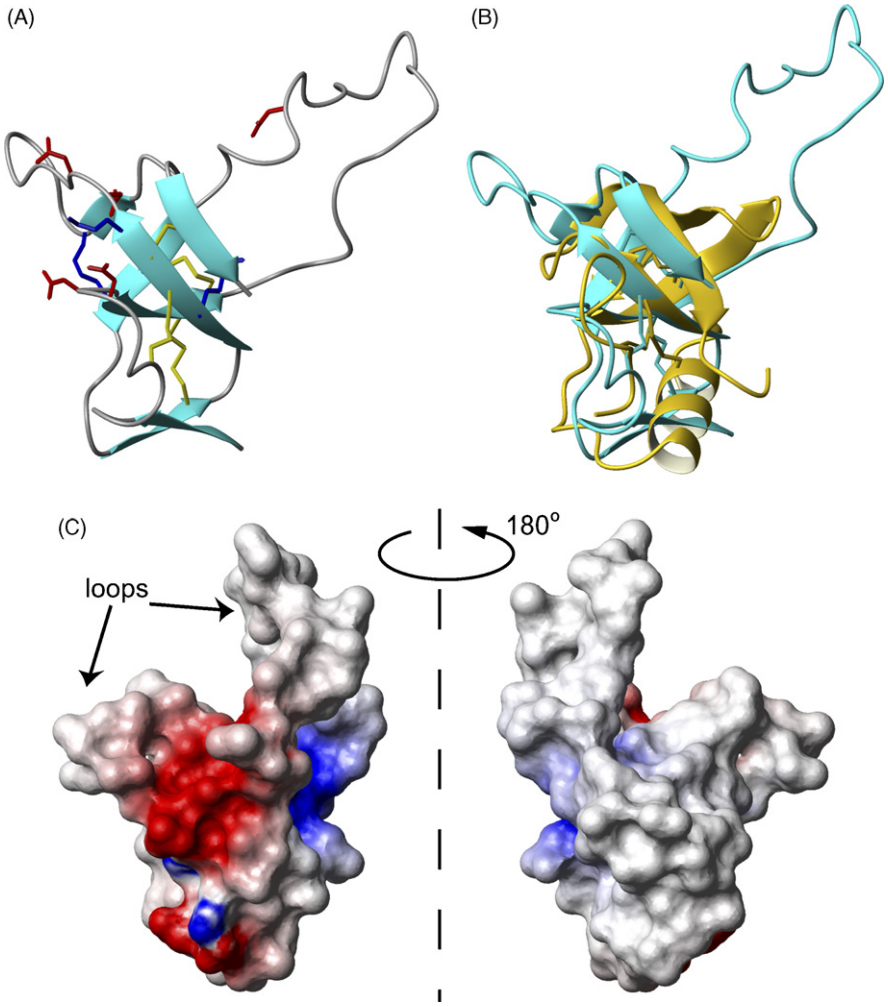

Fig. 5. Solution structure of EAS. (A) Ribbon diagram of EAS. Cys side chains are shown as yellow sticks while charged residues are shown as blue and red sticks. (B) Overlay of EAS (cyan) with HFBII (yellow). (C) Electrostatic surface of EAS. Uncharged residues are shown as grey and negatively and positively charged residues are illustrated in red and blue, respectively.

1979; Dempsey and Beever, 1979). Using surface replicas, freeze-fracture, and negative staining it was demonstrated that the rodlets formed a monolayer and were not interwoven or covered by another layer as had previously been suggested. (Fig. 2A and B). Evidence that the rodlet layer was responsible for imparting the hydrophobic properties to dry spores was obtained by comparing the surface of wild-type *N. crassa* spores to those of the easily wettable mutant (*eas*) (Selitrennikoff, 1976). The surface of the eas spores clearly lacked the mosaic of rodlets present on wild-type spores (Beever and Dempsey, 1978). Negative stained TEM images of purified EAS and SC3 rodlet layers suggest that the rodlets are either hollow or possess a groove running down the middle (Dempsey and Beever, 1979; Wessels, 1999; Gebbink et al., 2005). The rodlets have a diameter of ~10 nm and visible lengths ranging between 35 and 240 nm (Dempsey and Beever, 1979). The dimensions and morphology of the SC3 rodlets formed on aerial hyphae of *S. commune* are the same as those observed when the purified protein is dried down onto Formvar-coated TEM grids and when gas vesicles are coated with purified and polymerised SC3. It has also been demonstrated that the outer surface presented by the rodlets on native spores represents the hydrophobic face of the protein layer (Wösten et al., 1993).

4.2. X-ray studies and the similarities with amyloid

The structural and morphological similarities between class I rodlets and amyloid fibrils have been noted many times (for example, (Wösten and de Vocht, 2000; Stroud et al., 2003)) and SC3 and EAS rodlets both bind amyloid-specific dyes in a way that confirms that the core structure of these rodlets consists of stacked β-sheets. The soluble form of SC3 does not bind Thioflavin T, a fluorescent dye that is commonly used to detect the stacked β-structure of amyloid fibrils, but SC3 assembled into rodlets by vortexing gives rise to enhanced fluorescence when stained with the dye (Butko et al., 2001; Wang et al., 2005). EAS rodlets display the green-gold birefringence that is diagnostic for amyloid when stained with Congo red and viewed between cross-polarisers (Fig. 6A) (Mackay et al., 2001) and these rodlets also bind Thioflavin T (M. Sunde, unpublished data). Class II hydrophobin layers do not bind amyloid-specific dyes, indicating that they lack the stacked β-sheet structure

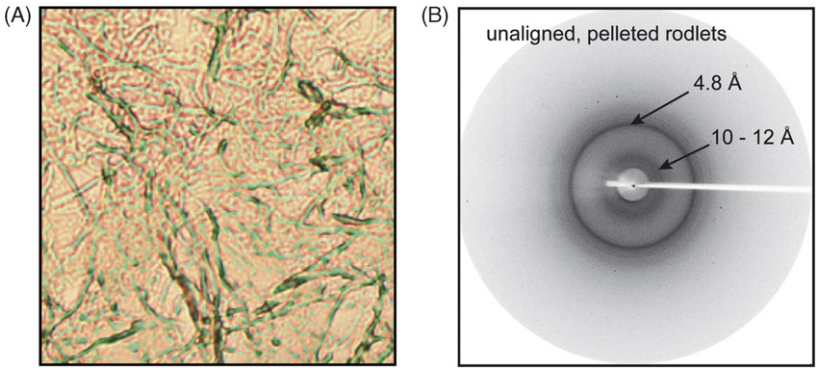

Fig. 6. Amyloid characteristics of hydrophobin rodlets. (A) Gold-green birefringence observed when EAS rodlets are stained with Congo red and viewed between cross-polarisers. (B) X-ray fibre diffraction image of unaligned, pelleted rodlets displays reflections at 4.8 and 10–12 Å, indicative of β-sheet structure.

recognised by these dyes (Torkkeli et al., 2002) and suggesting that significant structural differences at the level of monomer assembly underlie the morphological and physical differences between the class I and II rodlets.

X-ray diffraction studies of EAS rodlets confirm that they have an ordered β-structure core (Kwan et al., 2006). The diffraction pattern obtained from unaligned rodlets (produced by vortexing and then harvested by centrifugation) displays reflections at 4.8 and 10–12 Å, consistent with β-sheet structure (Fig. 6B). The pattern obtained from a monolayer rodlet film formed in a magnetic field additionally shows orientation of the inter-strand spacing and a spacing of ~27 Å that matches the diameter of the monomer. The lack of a prominent inter-sheet spacing in this pattern may be due to the fact that this is a monolayer sample.

Torkkeli and colleagues have shown that the class II hydrophobins HFBI and HFBII form fibrils on surfaces upon shaking of solutions (Torkkeli et al., 2002). Gentle mixing gives rise to regularly shaped HFBII fibrils that are 2–3 μm in diameter and 15–25 μm long. These HFBII aggregates have been examined by small and wide angle X-ray scattering (SAXS and WAXS) (Torkkeli et al., 2002) and grazing incidence X-ray diffraction (Ritva et al., 2003); the aggregates appear to have a monoclinic structure in solution and a hexagonal structure when dried, although the structural significance of these geometries is not currently clear. Notably, there is no reflection corresponding to 4.7–4.8 Å, indicating that there is no regular, repeated β-structure in these class II aggregates. The aggregates of HFBI that form under the same conditions are only weakly ordered and do not display any sharp diffraction peaks. One peak is observed in the diffraction pattern at ~15 Å that might arise from a short-range order of monomers (Ritva et al., 2003). SAXS intensities of concentrated solutions of HFBI and HFBII indicate that the defined aggregates consist of several protein chains (Torkkeli et al., 2002).

4.3. Imaging of hydrophobin films with atomic force microscopy

AFM studies of HFBI and HFBII films produced by the Langmuir–Blodgett technique show crystalline domains of the hydrophobins with regular features and a monolayer height of about 13 Å (Paananen et al., 2003). More recently, significant structural insight into class II hydrophobin films has been achieved with high resolution AFM studies of HFBI variants where the monolayer films have been probed from both the hydrophobic and hydrophilic sides (Szilvay et al., 2007). These class II hydrophobin layers do not have a rodlet-like morphology but instead display a striking hexagonal repeating pattern that arises spontaneously at the air–water interface (Fig. 7). The smallest observable repeating units have a diameter of about

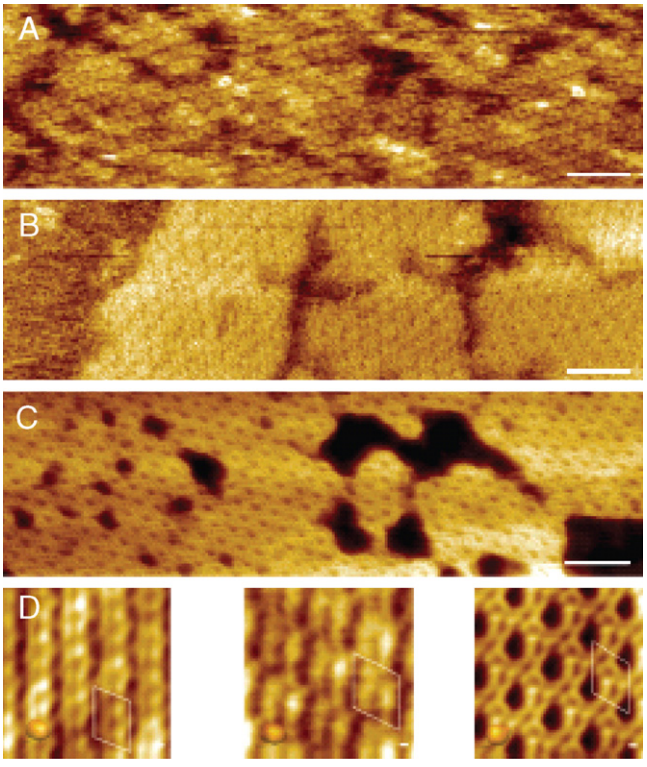

Fig. 7. AFM topography images of HFBI films. (A) Drop-surface film on highly oriented pyrolytic graphite results in hydrophilic surface towards the AFM probe, (B) film produced by Langmuir–Schaefer method and transferred to highly oriented pyrolytic graphite results in hydrophilic surface presented to the AFM probe, (C) film produced by Langmuir–Blodgett method and transferred to freshly cleaved mica results in hydrophobic surface presented to the AFM probe, and (D) correlation averages of single crystalline areas of (A) left, (B) middle and (C) right. Scale bars are 20 nm. Reprinted with permission from Szilvay et al. (2007), Copyright 2007 American Chemical Society.

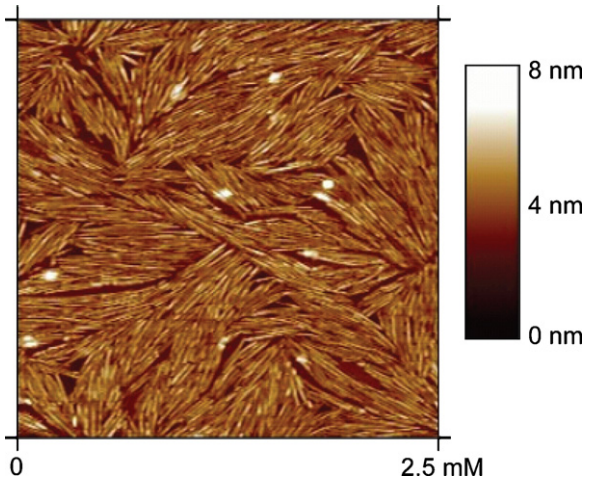

Fig. 8. Atomic force micrograph of rodlets formed by purified EAS. EAS solution at a concentration of 10 μg/ml was dried onto mica and imaged at room temperature in air. The scale indicates the height at each point.

5 nm and a surface area of 20–30 nm^2. Given the relative size of these units and the monomer of HFBI, each hexagonal unit is likely to represent an oligomeric assembly. HFBI labelled with biotin at the N-terminus did not yield high-resolution images in water, probably because of the flexibility of the linker but HFBI conjugated to biotin through the C-terminus gave good images. The addition of avidin from the hydrophilic side indicates the orientation of the protein within the amphipathic assembly and shows the potential for engineering of the surface properties of these hydrophobin monolayers.

All of these structural studies need to reconcile the models for hydrophobin conformation with the measured thickness of rodlets and class II hydrophobin layers. The thickness of the SC3 monolayer has been reported several times. de Vocht et al. (1998) used scanning force microscopy and estimated that the rodlets, which had an average diameter of 9–15 nm, were 7–8 nm thick. These results are in agreement with EM and other studies of class I hydrophobins, which generally report rodlet diameters for class I hydrophobins of about 10 nm (Dempsey and Beever, 1979) (Fig. 8). Wösten et al. (1994) have calculated that, on Teflon, the surface coating is about 28 nm^2/SC3 molecule and at the water–air interface it is 44 nm^2. SC3 would occupy ~7 nm^2 if spherical, suggesting that the protein adopts an extended conformation when it forms rodlets. In contrast, class II films may be thinner. As noted above, Paananen and coworkers have reported the thickness of a class II hydrophobin layer to be ~1.3 nm (Paananen et al., 2003). Szilvay et al. (2007) report thicknesses of 1.3–2.8 nm, depending on the manner of preparation of the film and conclude that the films are monomolecular layers, with the diameter of the globular, soluble form of HFBI being 2–3 nm.

5. Structural studies of the assembly process

Our current understanding of the conformational changes that take place upon self-association comes from spectroscopic techniques that are well suited to monitoring changes in secondary structure in proteins. CD and ATR FT-IR studies (de Vocht et al., 1998, 2002) both support the idea that SC3 undergoes a transition to a β-rich structure when polymerisation occurs at an interface. SC3 appears to initially populate a helix-rich conformation at the air–water interface, subsequently converting to the stable, β-rich rodlet form. Weak association of SC3 with Teflon can also induce a helix-rich state that is converted to the tightly bound β-form upon heating in the presence of detergent (Wösten and de Vocht, 2000). The class II hydrophobins HFBI and HFBII also display some increase in helical conformation when bound to Teflon but they do not undergo the conformational changes seen in SC3 when they assemble at an air–water interface (Askolin et al., 2005). Interestingly, the presence of intact native disulfide bridges does not appear to be essential for rodlet formation (de Vocht et al., 2000). SC3 reduced and treated with iodoacetamide (to methylate the cysteines and prevent re-formation of disulphides) underwent the same conformational changes detected for native SC3 and spontaneously formed native-like rodlets in water despite the lack of air–water interfaces. In contrast, reduction of the disulfide bonds and treatment with iodoacetic acid, which derivatizes the cysteine sidechains with a negatively charged carboxylate group, rendered SC3 unable to self-assemble into the β-rich form. These experiments suggest that the disulfide bridges are not directly involved in the assembly process but rather allow hydrophobins to assemble specifically at interfaces (de Vocht et al., 2000).

Polarisation-modulated infrared reflectance adsorption spectroscopy (PM-IRRAS) has been used to study the self-assembly of SC3 directly at the air–water interface (de Vocht et al., 2002). SC3 accumulates rapidly at the air–water interface and is seen to undergo a conformational transition from a mixture of secondary structure elements (band centred

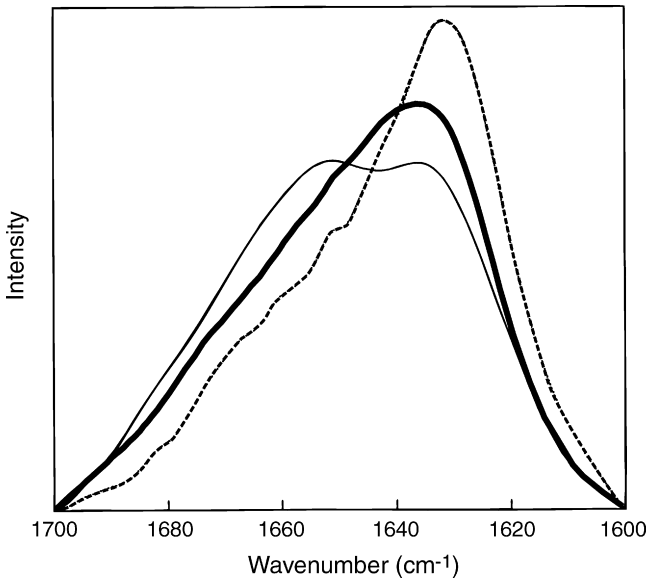

Fig. 9. Attenuated total reflectance Fourier-transform infra-red spectra of SC3 under a range of conditions: non-assembled SC3 deposited onto a germanium plate (dark thick line), vortexed SC3 on a germanium plate (dotted line), and vortexed SC3 on a silanized germanium plate which is subsequently heat-treated in 2% SDS (thin line). Vertical scale is arbitrary. Reprinted with permission from de Vocht et al. (1998), Copyright 1998 Biophysical Society.

at 1650 cm^{-1}) to a mainly β-sheet form (1631 cm^{-1} in H_2O and 1624 cm^{-1} in D_2O; Fig. 9). In addition, PM-IRRAS is able to give information about the orientation of secondary structure elements in a sample, relative to the incident surface. PM-IRRAS spectra from SC3 rodlets, collected from the interface surface, display a positive amide I band, indicating that the hydrogen bonds are oriented preferentially parallel to the air–water interface. Since the hydrogen bonds lie in the plane of the β-sheet, this indicates that the β-sheets in the SC3 rodlets are parallel to the surface and therefore also co-planar with the long axis of the rodlets. Studies of SC3 oligomerisation, monitored by EM and PM-IRRAS (de Vocht et al., 2002), suggest that accumulation of the hydrophobin at the interface to a critical concentration is necessary to allow rodlet formation and that conversion to the β-form takes place at the interface.

There have been several reports of hydrophobins forming oligomeric assemblies in solution. The idea that HFBI aggregates consist of multiple protein chains is supported by size exclusion chromatography (SEC) and SAXS data that imply that at high protein concentrations the main component is a tetramer. At lower protein concentrations, monomers (HFBII) and dimers (HFBI) are also observed (Torkkeli et al., 2002). The same group has recently used Főrster resonance energy transfer (FRET) with N-terminally labelled HFBI to study self-assembly of these hydrophobins (Szilvay et al., 2006). The formation of the tetramers in solution appears to be cooperative and driven by the hydrophobic effect. Although tetramer formation in solution might represent a nucleation event on the pathway to higher order assemblies, the fact that the hydrophobic surface is likely to be buried in these structures indicates that such tetramers would have to disassemble at an interface and rearrange to form an amphipathic film. Indeed, recent results demonstrate that, at least for HFBI, a shift in the equilibrium towards the tetramer does not significantly alter the surface activity of the protein (Szilvay et al., 2007). Similarly, Stroud and co-workers have characterised a multimeric, non-rodlet, SDS-insoluble state of SC3 in solution, which can be converted to the rodlet form by vortexing (Stroud et al., 2003). These multimeric forms may be similar to the oligomeric SC3 intermediates reported by (Wang et al., 2004). In contrast, the class I hydrophobin EAS exists mainly as a monomer in solution as determined by equilibrium sedimentation and NMR studies (Mackay et al., 2001).

While there are similarities in the structures of the soluble forms of hydrophobins and the function of the polymerised films, the different intermediate oligomerisation states detected may reflect differences in the individual protein sequences and consequently, distinct pathways that hydrophobin molecules may take to form the final assembled hydrophobin film.

6. Conclusions

Hydrophobins are a class of proteins with striking physical properties. A detailed understanding of the molecular mechanisms underlying these properties is of great interest from an academic perspective but perhaps is even more relevant from a commercial viewpoint. Not only are hydrophobins an integral component of many fungi, but also considerable opportunities exist for the rational design of hydrophobins for nano and biotechnological applications. The progress made in the amyloid field over the last 10 years suggests that a full understanding of the structural basis for rodlet formation might be most likely to come from a multi-faceted approach that involves the analysis of both monomeric and polymeric forms using a wide range of microscopic and spectroscopic techniques. A substantial amount of data exists for a number of hydrophobins already, and it is quite possible that we will see significant advances made over the next 5 years.

References

Askolin, S., Penttila, M., Wosten, H.A.B., Nakari-Setala, T., 2005. The *Trichoderma reesei* hydrophobin genes *hfb1* and *hfb2* have diverse functions in fungal development. FEMS Microbiol. Lett. 253, 281–288.

Beever, R.E., Dempsey, G.P., 1978. Function of rodlets on the surface of fungal spores. Nature 272, 608–610.

Beever, R.E., Redgwell, R.J., Dempsey, G.P., 1979. Purification and chemical characterization of the rodlet layer of *Neurospora crassa* conidia. J. Bacteriol. 140, 1063–1070.

Bell-Pedersen, D., Dunlap, J.C., Loros, J.J., 1992. The Neurospora circadian clock-controlled gene, *ccg-2*, is allelic to *eas* and encodes a fungal hydrophobin required for formation of the conidial rodlet layer. Genes Dev. 6, 2382–2394.

Bowden, C.G., Smalley, E., Guries, R.P., Hubbes, M., Temple, B., Horgan, P.A., 1996. Lack of association between cerato-ulmin production and virulence in Ophiostoma novo-ulmi. Mol. Plant Microbe Interact. 9, 556–564.

Brasier, C.M., Kirk, S.A., Tegli, S., 1995. Naturally-occurring non-cerato-ulmin producing mutants of ophiostoma-novo-ulmi are pathogenic but lack aerial mycelium. Mycol. Res. 99, 436–440.

Butko, P., Buford, J.P., Goodwin, J.S., Stroud, P.A., McCormick, C.L., Cannon, G.C., 2001. Spectroscopic evidence for amyloid-like interfacial self-assembly of hydrophobin Sc3. Biochem. Biophys. Res. Commun. 280, 212–215.

Claessen, D., Rink, R., de Jong, W., Siebring, J., de Vreugd, P., Boersma, F.G.H., Dijkhuizen, L., Wösten, H.A.B., 2003. A novel class of secreted hydrophobic proteins is involved in aerial hyphae formation in *Streptomyces coelicolor* by forming amyloid-like fibrils. Genes Dev. 17, 1714–1726.

Cole, G.T., 1973. A correlation between rodlet orientation and conidiogenesis in Hyphomycetes. Can.J. Bot. 51, 2413–2422.

de Vocht, M.L., Scholtmeijer, K., van der Vegte, E.W., de Vries, O.M.H., Sonveaux, N., Wosten, H.A.B., Ruysschaert, J.M., Hadziioannou, G., Wessels, J.G.H., Robillard, G.T., 1998. Structural characterization of the hydrophobin SC3, as a monomer and after self-assembly at hydrophobic/hydrophilic interfaces. Biophys. J. 74, 2059–2068.

de Vocht, M.L., Reviakine, I., Wosten, H.A.B., Brisson, A., Wessels, J.G.H., Robillard, G.T., 2000. Structural and functional role of the disulfide bridges in the hydrophobin SC3. J. Biol. Chem. 275, 28428–28432.

de Vocht, M.L., Reviakine, I., Ulrich, W.P., Bergsma-Schutter, W., Wosten, H.A.B., Vogel, H., Brisson, A., Wessels, J.G.H., Robillard, G.T., 2002. Self-assembly of the hydrophobin SC3 proceeds via two structural intermediates. Protein Sci. 11, 1199–1205.

de Vries, O.M.H., Fekkes, M.P., Wösten, H.A.B., Wessels, J.G.H., 1993. Insoluble hydrophobin complexes in the walls of *Schizophyllum commune* and other filamentous fungi. Arch. Microbiol. 159.

Dempsey, G.P., Beever, R.E., 1979. Electron microscopy of the rodlet layer of *Neurospora crassa* conidia. J. Bacteriol. 140, 1050–1062.

Dons, J.J.M., Springer, J., de Vries, S.C., Wessels, J.G.H., 1984. Molecular cloning of a gene abundantly expressed during fruiting body initiation in *Schizophyllum commune*. J. Bacteriol. 157, 802–808.

Gebbink, M.F.B.G., Claessen, D., Bouma, B., Dijkhuizen, L., Wösten, H.A.B., 2005. Amyloids-a functional coat for microorganisms. Nat. Rev. (Microbiol.) 3, 333–341.

Please cite this article in press as: Sunde, M., et al., Structural analysis of hydrophobins, Micron (2007), doi:10.1016/j.micron.2007.08.003

Ghiorse, W., Edwards, M., 1973. Ultrastructure of *Aspergillus fumigatus* conidia development and maturation. Protoplasma 76, 49–59.

Hakanpää, J., Parkkinen, T.A.A., Hakulinen, N., Linder, M., Rouvinen, J., 2004a. Crystallization and preliminary X-ray characterization of *Trichoderma reesei* hydrophobin HFBII. Acta Crystallogr. D: Biol. Crystallogr. 60, 163–165.

Hakanpää, J., Paananen, A., Askolin, S., Nakari-Setala, T., Parkkinen, T., Penttila, M., Linder, M.B., Rouvinen, J., 2004b. Atomic resolution structure of the HFBII hydrophobin, a self-assembling amphiphile. J. Biol. Chem. 279, 534–539.

Hakanpää, J., Linder, M., Popov, A., Schmidt, A., Rouvinen, J., 2006a. Hydrophobin HFBII in detail: ultrahigh-resolution structure at 0.75 angstrom. Acta Crystallogr. D: Biol. Crystallogr. 62, 356–367.

Hakanpää, J., Szilvay, G.R., Kaljunen, H., Maksimainen, M., Linder, M., Rouvinen, J., 2006b. Two crystal structures of *Trichoderma reesei* hydrophobin HFBI—The structure of a protein amphiphile with and without detergent interaction. Protein Sci. 15, 2129–2140.

Hess, W.H., Sassen, M.M.A., Remsen, C.C., 1968. Surface characteristics of Penicillum conidia. Mycologia 60, 291–303.

Hess, W.M., Bushnell, J.L., Weber, D.J., 1969. Surface characteristics of Aspergillus conidia. Mycologia 61, 560–571.

Hobot, J.A., Gull, K., 1981. Structure and biochemistry of the spore surface of *Syncephalastrum racemosum*. Curr. Microbiol. 5, 183–185.

Janssen, M.I., van Leeuwen, M.B.M., van Kooten, T.G., de Vries, J., Dijkhuizen, L., Wosten, H.A.B., 2004. Promotion of fibroblast activity by coating with hydrophobins in the beta-sheet end state. Biomaterials 25, 2731–2739.

Kazmierczak, P., Kim, D.H., Turina, M., Van Alfen, N.K., 2005. A hydrophobin of the chestnut blight fungus, *Cryphonectria parasitica*, is required for stromal pustule eruption. Eukaryot. Cell 4, 931–936.

Kershaw, M.J., Talbot, N.J., 1998. Hydrophobins and repellents: proteins with fundamental roles in fungal morphogenesis. Fungal Genet. Biol. 23, 18–33.

Kim, S., Ahn, I.-P., Rho, H.-S., Lee, Y.-H., 2005. MHP1, a *Magnaporthe grisea* hydrophobin gene, is required for fungal development and plant colonization. Mol. Microbiol. 57, 1224–1237.

Kwan, A., Winefield, R.D., Sunde, M., Matthews, J.M., Haverkamp, R.G., Templeton, M.D., Mackay, J.P., 2006. Structural basis for rodlet assembly in fungal hydrophobins. Proc. Natl. Acad. Sci. U.S.A. 103, 3621–3626.

Linder, M., Szilvay, G.R., Nakari-Setala, T., Soderlund, H., Penttila, M., 2002. Surface adhesion of fusion proteins containing the hydrophobins HFBI and HFBII from *Trichoderma reesei*. Protein Sci. 11, 2257–2266.

Linder, M.B., Qiao, M.Q., Laumen, F., Selber, K., Hyytia, T., Nakari-Setala, T., Penttila, M.E., 2004. Efficient purification of recombinant proteins using hydrophobins as tags in surfactant-based two-phase systems. Biochemistry 43, 11873–11882.

Linder, M.B., Szilvay, G.R., Nakari-Setala, T., Penttila, M.E., 2005. Hydrophobins: the protein-amphiphiles of filamentous fungi. FEMS Microbiol. Rev. 29, 877–896.

Lugones, L.G., Wosten, H.A.B., Birkenkamp, K.U., Sjollema, K.A., Zagers, J., Wessels, J.G.H., 1999. Hydrophobins line air channels in fruiting bodies of *Schizophyllum commune* and *Agaricus bisporus*. Mycol. Res. 103, 635–640.

Mackay, J.P., Matthews, J.M., Winefield, R.D., Mackay, L.G., Haverkamp, R.G., Templeton, M.D., 2001. The hydrophobin EAS is largely unstructured in solution and functions by forming amyloid-like structures. Structure 9, 83–91.

Martin, F., Laurent, P., Decarvalho, D., Burgess, T., Murphy, P., Nehls, U., Tagu, D., 1995. Fungal gene-expression during ectomycorrhiza formation. Can. J. Bot. (Revue Canadienne De Botanique) 73, S541–S547.

Martin, F., Laurent, P., de Carvalho, D., Voiblet, C., Balestrini, R., Bonfante, P., Tagu, D., 1999. Cell wall proteins of the ectomycorrhizal basidiomycete *Pisolithus tinctorius*: identification, function, and expression in symbiosis. Fungal Genet. Biol. 27, 161–174.

Paananen, A., Vuorimaa, E., Torkkeli, M., Penttila, M., Kauranen, M., Ikkala, I., Lemmetyinen, H., Serimaa, R., Linder, M.B., 2003. Structural hierarchy in molecular films of two class II hydrophobins. Biochemistry 42, 5253–5258.

Qin, M., Wang, L., Feng, X., Yang, Y., Wang, R., Wang, C., Yu, L., Shao, B., Qiao, M., 2007. Bioactive surface modification of mica and poly(dimethylsiloxane) with hydrophobins for protein immobilization. Langmuir.

Rillig, M.C., 2005. A connection between fungal hydrophobins and soil water repellency? Pedobiologia 49, 395–399.

Ritva, S., Torkkeli, M., Paananen, A., Linder, M., Kisko, K., Knaapila, M., Ikkala, O., Vuorimaa, E., Lemmetyinen, H., Seeck, O., 2003. Self-assembled structures of hydrophobins HFBI and HFBII. J. Appl. Crystallogr. 36, 499–502.

Sassen, M., Remsen, C., Hess, W., 1967. Fine structure of *Penicillium megasporum* conidiophores. Protoplasma 64, 75–88.

Scherrer, S., De Vries, O.M.H., Dudler, R., Wessels, J.G.H., Honegger, R., 2000. Interfacial self-assembly of fungal hydrophobins of the lichen-forming ascomycetes *Xanthoria parietina* and X-ectaneoides. Fungal Genet. Biol. 30, 81–93.

Scherrer, S., Haisch, A., Honegger, R., 2002. Characterization and expression of XPH1, the hydrophobin gene of the lichen-forming ascomycete *Xanthoria parietina*. New Phytologist 154, 175–184.

Selitrennikoff, C.P., 1976. Easily-wettable, a new mutant. Neurospora News lett. 23, 23.

Spanu, P., 1998. Deletion of HCf-1, a hydrophobin gene of *Cladosporium fulvum*, does not affect pathogenicity in tomato. Physiol. Mol. Plant Pathol. 52, 323–334.

Stringer, M.A., Dean, R.A., Sewall, T.C., Timberlake, W.E., 1991. *Rodletless*, a new *Aspergillus* developmental mutant induced by directed gene inactivation. Genes Dev. 5, 1161–1171.

Stroud, P.A., Goodwin, J.S., Butko, P., Cannon, G.C., McCormick, C.L., 2003. Experimental evidence for multiple assembled states of Sc3 from *Schizophyllum commune*. Biomacromolecules 4, 956–967.

Szilvay, G.R., Nakari-Setala, T., Linder, M.B., 2006. Behavior of *Trichoderma reesei* hydrophobins in solution: interactions, dynamics, and multimer formation. Biochemistry 45, 8590–8598.

Szilvay, G.R., Paananen, A., Laurikainen, K., Vuorimaa, E., Lemmetyinen, H., Peltonen, J., Linder, M.B., 2007. Self-assembled hydrophobin protein films at the air–water interface: structural analysis and molecular engineering. Biochemistry 46, 2345–2354.

Tagu, D., Kottke, I., Martin, F., 1998. Hydrophobins in ectomycorrhizal symbiosis: hypothesis. Symbiosis 25, 5–18.

Tagu, D., Marmeisse, R., Baillet, Y., Riviere, S., Palin, B., Bernardini, F., Mereau, A., Gay, G., Balestrini, R., Bonfante, P., Martin, F., 2002. Hydrophobins in ectomycorrhizas: heterologous transcription of the Pisolithus HydPt-1 gene in yeast and *Hebeloma cylindrosporum*. Eur. J. Histochem. 46, 23–29.

Talbot, N.J., Kershaw, M.J., Wakley, G.E., deVries, O.M.H., Wessels, J.G.H., Hamer, J.E., 1996. MPG1 encodes a fungal hydrophobin involved in surface interactions during infection-related development of *Magnaporthe grisea*. Plant Cell 8, 985–999.

Teertstra, W.R., Deelstra, H.J., Vranes, M., Bohlmann, R., Kahmann, R., Kamper, J., Wosten, H.A.B., 2006. Repellents have functionally replaced hydrophobins in mediating attachment to a hydrophobic surface and in formation of hydrophobic aerial hyphae in *Ustilago maydis*. Microbiology 152, 3607–3612.

Temple, B., Horgen, P.A., 2000. Biological roles for cerato-ulmin, a hydrophobin secreted by the elm pathogens, Ophiostoma ulmi and O-novo-ulmi. Mycologia 92, 1–9.

Torkkeli, M., Serimaa, R., Ikkala, O., Linder, M., 2002. Aggregation and self-assembly of hydrophobins from *Trichoderma reesei*: low-resolution structural models. Biophys. J. 83, 2240–2247.

Trembley, M.L., Ringli, C., Honegger, R., 2002. Differential expression of hydrophobins DGH1, DGH2 and DGH3 and immunolocalization of DGH1 in strata of the lichenized basidiocarp of *Dictyonema glabratum*. New Phytologist 154, 185–195.

van Wetter, M.A., Wosten, H.A.B., Wessels, J.G.H., 2000. SC3 and SC4 hydrophobins have distinct roles in formation of aerial structures in dikaryons of *Schizophyllum commune*. Mol. Microbiol. 36, 201–210.

Wang, X., De Vocht, M.L., De Jonge, J., Poolman, B., Robillard, G.T., 2002. Structural changes and molecular interactions of hydrophobin SC3 in solution and on a hydrophobic surface. Protein Sci. 11, 1172–1181.

Wang, X., Permentier, H.P., Rink, R., Kruijtzer, J.A.W., Liskamp, R.M.J., Wosten, H.A.B., Poolman, B., Robillard, G.T., 2004. Probing the self-assembly and the accompanying structural changes of hydrophobin SC3 on a hydrophobic surface by mass spectrometry. Biophys. J. 87, 1919–1928.

Please cite this article in press as: Sunde, M., et al., Structural analysis of hydrophobins, Micron (2007), doi:10.1016/j.micron.2007.08.003

Wang, X., Shi, F.X., Wosten, H.A.B., Hektor, H., Poolman, B., Robillard, G.T., 2005. The SC3 hydrophobin self-assembles into a membrane with distinct mass transfer properties. Biophys. J. 88, 3434–3443.

Wessels, J.G.H., 1994. Developmental regulation of fungal cell-wall formation. Ann Rev. Phytopathol. 32, 413–437.

Wessels, J.G.H., 1996. Fungal hydrophobins: proteins that function at an interface. Trends Plant Sci. 1, 9–15.

Wessels, J.G.H., 1999. Fungi in their own right. Fungal Genet. Biol. 27, 134–145.

Wessels, J.G.H., de Vries, O.M.H., Asgeirsdottir, S.A., Schuren, F.H.J., 1991. Hydrophobin genes involved in formation of aerial hyphae and fruit bodies in Schizophyllum. Plant Cell 3, 793–799, doi:10.1105/tpc.3.8.793.

Whiteford, J.R., Spanu, P.D., 2001. The hydrophobin HCf-1 of *Cladosporium fulvum* is required for efficient water-mediated dispersal of conidia. Fungal Genet. Biol. 32, 159–168.

Whiteford, J.R., Lacroix, H., Talbot, N.J., Spanu, P.D., 2004. Stage-specific cellular localisation of two hydrophobins during plant infection by the pathogenic fungus *Cladosporium fulvum*. Fungal Genet. Biol. 41, 624–634.

Wösten, H.A.B., 2001. Hydrophobins: multipurpose proteins. Ann. Rev. Microbiol. 55, 625–646.

Wösten, H.A.B., de Vocht, M.L., 2000. Hydrophobins, the fungal coat unravelled. Biochim. Biophys. Acta Rev. Biomembr. 1469, 79–86.

Wösten, H.A.B., Devries, O.M.H., Wessels, J.G.H., 1993. Interfacial self-assembly of a fungal hydrophobin into a hydrophobic rodlet layer. Plant Cell 5, 1567–1574.

Wösten, H.A.B., Asgeirsdottir, S.A., Krook, J.H., Drenth, J.H.H., Wessels, J.G.H., 1994. The fungal hydrophobin Sc3p self-assembles at the surface of aerial hyphae as a protein membrane constituting the hydrophobic rodlet layer. Eur. J. Cell Biol. 63, 122–129.

Wösten, H.A.B., van Wetter, M.A., Lugones, L.G., van der Mei, H.C., Busscher, H.J., Wessels, J.G.H., 1999. How a fungus escapes the water to grow into the air. Curr. Biol. 9, 85–88.

Yaguchi, M., Pusztai-Cary, M., Roy, C., Surewicz, W.K., Carey, P.R., Stevenson, K.J., Richards, W.C., Takai, S., 1993. Amino acid sequence and spectroscopic studies of Dutch elm disease toxin, ceratoulmin. In: Sticklen, M.B., Sherald, J.L. (Eds.), Dutch Elm Disease Research: Cellular and Molecular Approaches. 1st ed. Springer-Verlag, New York, pp. 152–170.

Zhao, Z.-X., Qiao, M.-Q., Yin, F., Shao, B., Wu, B.-Y., Wang, Y.-Y., Wang, X.-S., Qin, X., Li, S., Yu, L., Chen, Q., 2007. Amperometric glucose biosensor based on self-assembly hydrophobin with high efficiency of enzyme utilization. Biosens. Bioelectron. 22, 3021–3027.

Please cite this article in press as: Sunde, M., et al., Structural analysis of hydrophobins, Micron (2007), doi:10.1016/j.micron.2007.08.003